

Development of effective sealing units for oil and gas equipment in the oil and gas production system

Opracowanie skutecznych zespołów uszczelniających dla urządzeń naftowych w systemie wydobywczym ropy i gazu

Ilman I. Hasanov, Agali A. Guliyev

Azerbaijan State Oil and Industry University

ABSTRACT: The paper presents the results of many years of experience in studying the efficiency of sealing units in the conditions of their operation in the oil and gas production system, as well as the influence of technological parameters that ensure normal operation and protect them from failure due to leakage through the working surface of the seals in the friction zone. In addition, according to the results of practical studies, it has been established that, in order to improve the elastic properties, for example, of cup springs of a direct-flow valve, we calculated heat treatment of the operational values of spring compression for various material thicknesses. The work of the elastic elements of the packer was improved mainly by the design, and the optimal parameters for the development of the elastic element of the packer were determined. The study of the stress-strain state of the sealing element of packers during setting and improving its performance is of both practical and scientific interest. One of the factors that significantly affect operation of pumps is the fluid leakage in valve assemblies in order to identify the effect of the above parameters on tightness based on a preliminary theoretical analysis. Comparison of data during the study showed that the flow rate of work with low viscosities is greater than with high viscosities. The technological processes of hardening the parts of the shut-off assembly of X-mas tree valves, to increase their reliability, are considered. The dependence of the compression force of the spring and its deformation because of geometric parameters of the disk springs has been determined; it has been found that the residual deformation of the disk spring after collapse has a negative effect on tightness. Calculations show that the amount of leakage of the elastic elements in the sealing assembly should not exceed ≤ 0.309 , since the seal at the value of elastic energy deformation provides a self-compacting mode. Thus, the degree of uneven pressing of the seat to the surface of the gate and its regulation to prevent leakage is practically determined.

Key words: oil and gas equipment, sealing element, stress-strain state, tightness, self-sealing, seizing value, force-deformation, physical wear, durability.

STRESZCZENIE: Artykuł przedstawia wyniki wieloletnich doświadczeń w badaniu skuteczności zespołów uszczelniających, w warunkach ich pracy w systemie wydobywczym ropy i gazu, jak również wpływ parametrów technologicznych zapewniających ich normalną eksploatację i zabezpieczających je przed awarią spowodowaną wyciekami przez powierzchnię roboczą uszczelnienia w strefie tarcia. Ponadto, zgodnie z wynikami badań o charakterze praktycznym, ustalono, że aby poprawić właściwości sprężyste, np. sprężyn talerzowych zaworu bezpośredniego przepływu, obliczono obróbkę cieplną wartości eksploatacyjnych ściśnięcia sprężyny dla różnych grubości materiału. Praca elementów sprężystych uszczelnacza została poprawiona głównie dzięki projektowi oraz ustalono optymalne parametry dla budowy elementu sprężystego uszczelnacza. Badania stanu naprężenie-odkształcenie elementu uszczelniającego uszczelnacza w czasie posadowienia oraz poprawa jego działania są interesujące zarówno ze względów praktycznych, jak i naukowych. Jednym z czynników znacząco wpływających na pracę pomp jest wyciek płynu w zespołach zaworów, co pozwoliło na określenie wpływu powyższych parametrów na szczelność w oparciu o wstępną analizę teoretyczną. Porównanie danych w czasie badania wykazało, że prędkość przepływu pracy z niskimi lepkościami jest większa niż z wysokimi lepkościami. Rozważane są procesy technologiczne utwardzania części zespołu odcinającego zaworów choinkowych w celu zwiększenia ich niezawodności. Ustalono zależność siły ściskania sprężyny i jej odkształcenia ze względu na parametry geometryczne sprężyn talerzowych; stwierdzono, że odkształcenie resztkowe sprężyny talerzowej po zgnieceniu ma negatywny wpływ na szczelność. Obliczenia wykazują, że wielkość wycieku elementów sprężystych w zespole uszczelniającym nie powinna przekraczać $\leq 0,309$, gdyż uszczelnienie przy wartości odkształcenia energii sprężystej zapewnia tryb samoczynnego zagęszczania. Tak więc stopień nierównomiernego dociśnięcia gniazda do powierzchni zasuwki i jego regulacja w celu przeciwdziałania wyciekowi został praktycznie określony.

Słowa kluczowe: urządzenia przemysłu naftowego, element uszczelniający, stan naprężenie-odkształcenie, samuszczelnianie, wartość zatarcia, siła-odkształcenie, zużycie fizyczne, trwałość.

Corresponding author: I.I. Hasanov, e-mail: hesenov.74@inbox.ru

Article contributed to the Editor: 09.01.2023. Approved for publication: 30.06.2023.

Object of study

Sealing element of downhole packers; valves of sucker-rod deep borehole pumps, some parts of the shut-off unit of a direct-flow valve.

Introduction

Studying the sealing assembly and its stress-strain state in the contact zone, ensuring its tightness and clarifying physical wear, i.e., the value of the worn layer (in microns) in order to increase the durability, efficiency and reliability of their operation in oil and gas equipment.

Problem statement

Numerous studies have shown that physical wear of individual parts (assemblies) of the sealing part of a machine or equipment under the influence of friction is characterized by three successive stages (Figure 1): intensive wear during the running-in period, section 1; a slower increase in wear during normal operation, section 2, and a progressive increase in wear after it reaches its maximum value, section 3.

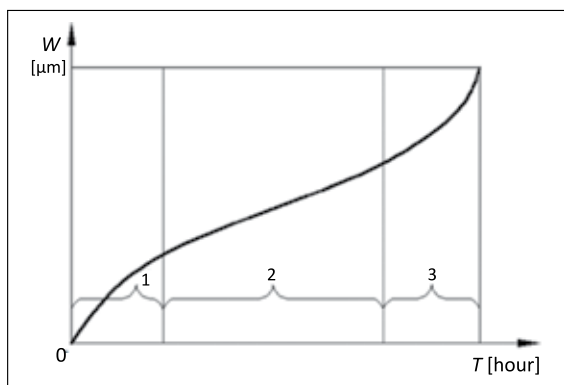


Figure 1. Wear curve of sealing parts of machinery and equipment under the action of friction according to the IT diagram; 1 – running-in period, 2 – period of normal operation, 3 – period of intensive wear, W – value of wear [microns], T – the duration of work [hour]

Rysunek 1. Krzywa zużycia części uszczelniających maszyn i urządzeń pod działaniem tarcia zgodnie z wykresem W - T ; 1 – okres rozruchu, 2 – okres normalnej pracy, 3 – okres intensywnego zużycia, W – wartość zużycia [mikrony], T – czas trwania pracy [godziny]

At the same time, the regularities of physical wear of sealing units' parts, the destruction of which occurs not under the influence of operational friction, but for various other reasons, for example, due to metal fatigue, a sudden stoppage of the supply of lubricating oil to the friction zone of parts

and exposure to aggressive media, are much less studied. The regularities of physical wear and tear of rubbing sections of machines and equipment as a whole have been studied even less; this task is more difficult at the same time more interesting for future research.

Problem solution

It is known from field practice that the wear of oil and gas field machines and equipment leads to defects in units and parts, as well as an increase in the consumption of operating materials. There comes a time when the further operation of the machine becomes economically and technically inexpedient. With a sufficiently large physical deterioration of the equipment, they either stop working, or signs of a serious technical accident occur. During the operation of oil and gas equipment and units, the maintenance personnel are constantly subjected to monitoring violations in the sealing density of the piston rod and stuffing box as not equipped with a system for removing leaks from the leak zone, as well as others equipped with such a system. An indicator of the tightness of the seals of the rods of compressors or pumps is the leakage of gas or oil in controlled places in the working places.

At each repair of oil and gas equipment (compressors, pumps, etc.), the condition of the seals is checked for the appearance of deep scuffs and cracks or breakage of any of the elements that require urgent replacement. In reciprocating and centrifugal compressor machines and pumps, there are sealing rings that are checked for wear on working surfaces, namely the cylinder mirror, piston, and ring, as well as between the rod and the supporting wall of the cylinder. In the case of more than 0.15–0.2 mm wear, replacing the rings and polishing the mirror part of the cylinder is required. The service personnel, moving the ring in the inner part of the housing, checks whether there has been a weakening of its fit. Signs of local defects (scuffs, nicks, scratches in the cylinder mirror, small cracks in the ring) should not occupy an area of more than 8–10% of the working surface, and the surface roughness is not permitted beyond 0.2 mm. Sealing split rings with an overlap are used with a plate spring, having a thickness of a strip steel spring of 1–1.5 mm, to create an increased tightness of the seal between the piston and the cylinder. For this, in oil and gas field practice, for finished sealing piston rings, before installation in piston compressor machines, the pressure value (P) of the clamp and the accuracy of fit to the compressor cylinder mirror are determined according to the formula:

$$P = 0.76 Q / D \cdot t' \quad (1)$$

where: Q – is the concentrated pressure load of the gas flow when the ring is compressed to the thermal gap on the

cylinder mirror, D – is the diameter of the compressor cylinder and t – is the height of the ring, both taken from the manufacturer's instructions.

Table 1. Operating pressures of the piston sealing rings

Tabela 1. Ciśnienia robocze pierścieni uszczelniających tłoka

Operating pressure, Q [MPa]	Cylinder diameter, D [mm]	Ring clamping pressure, P [MPa]
To 5	300–350	0.018–0.030
To 10	350–200	0.030–0.040
Above 10	200–100	0.040–0.050

The magnitude of the applied load can be easily measured using a conventional spring balance. For practical purposes, the operating pressures of the piston sealing rings are given in Table 1, depending on the operating pressure of the compressed gas and the cylinder diameter.

Problem solution method

Modern oil and gas equipment is characterized by a significant variety of machine and equipment designs, due to an extremely wide range of technological functions, both in drilling and in the operation of oil and gas wells.

Under conditions of high temperature and aggressive environments, such as for boosting and transporting to the gas lift system and to the consumer with high pressure, associated petroleum gas of medium and low pressure, containing acidic components without lubrication of compressor cylinders, polymers, based on Fluoroplast 4B and Fluoroplast 40P, showed a high level of exploitation. The use of composite materials 4B and 40P made it possible not only to increase the operation factor of compressor machines, but also to reduce the wear of cylinder liners, piston grooves and sealing rings, and to increase operational reliability, as well as to reduce the running-in time during the start-up period. Based on Fluoroplast 4V and 40R, sealing piston rings have been developed and manufactured, which have shown efficiency when working with piston compressors in dry friction. Table 2 shows some of the positive positions of Fluoroplast 4B and 40P based composite materials used as sealing rings.

As can be seen from Table 2, some composite materials, based on Fluoroplast 4B and 40P, used in oil and gas companies both offshore and onshore in gas lift and air lift systems, have shown efficiency and reliability in operation.

It should be noted that the improvement of the performance of the sealing elements of a two-pass packer operated in oil and gas wells was previously carried out mainly partially con-

Table 2. Beneficial properties of Fluoroplast 4B and 40P based composite materials used as sealing rings

Tabela 2. Korzystne właściwości materiałów kompozytowych na bazie Fluoroplastu 4B i 40P używanych jako pierścienie uszczelniające

Material Grade	Binder	Fillers [%]	Filler content [% (wt.)]
4K20	Fluoroplast 4B	coke powder; graphite + molybdenum disulfide; graphite + molybdenum disulfide + fiberglass; Steel J3+ molybdenum disulfide; graphite	20; 8; 35; 33; 15
Φ40Q10	Fluoroplast 40P	graphite; molybdenum disulfide	30; 30

structively, and the issues related to determining the optimal parameters for the development of more highly efficient elastic elements of a two-pass packer are incompletely studied.

As an example, to determine the optimal technological parameters of the elastic element of the seal, we used the dimensionless coefficient ψ_s , which characterizes the geometric shape of the element and is determined by the formula (Disk springs, 2003):

$$\psi_s = \frac{S - 2S_{s,c}}{S_w} \tag{2}$$

where: $S = \pi R^2 - \pi(r_1^2 + r_2^2)$ – the area of the supporting surface of the elastic element, R – is the radius of the circumference of the profile of the elastic element, r_1, r_2 – are the radii of passage holes, $S_{s,c}$ – is the supporting surface of the cutout at the ends of the elastic element, S_w – is the loading area of the support washer with a diameter – D_2 , provided in the sealing assembly of the two-pass packer.

The available cutout in the design of the packer's elastic element is a volume cut out in the body of the seal (from the supporting and side surfaces), with a radius R from the center O and a radius R_1 from the centre O_1 (Figure 2) (Babanli, 2016).

Improving the performance of the sealing element of packers is possible only after establishing the relationship between its technological parameters and the efficiency of the sealer during well operation. Consider simultaneously the two-sided compression of the sealing element of the packers.

Here, the first stage of deformation will be studied, i.e., deformation of the sealing element of the loading part until its middle touches the casing string wall. At the same time, due to the presence of thrust washers, we accept geometric figures as flat sections.

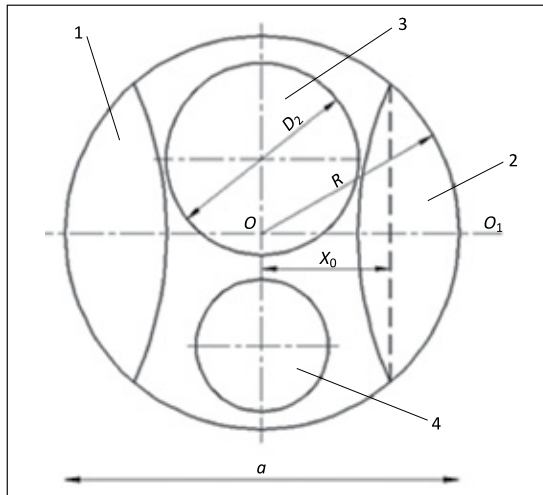


Figure 2. Scheme for determining the geometric characteristics of the elastic element of the packer seal; 1, 2 – volumes extracted from the elastic element, 3, 4 – eccentric holes

Rysunek 2. Schemat dla ustalania właściwości geometrycznych elementu sprężystego uszczelki uszczelniaacza; 1, 2 – objętości uzyskane z elementu sprężystego, 3, 4 – otwory niewspółśrodkowe

In this case, the deformation of the sealing element (ω) is taken as a function of the Z coordinate (Figure 3):

$$\omega = \psi(z) \quad (3)$$

where: $\psi(z)$ – geometric characteristic of the elastic element, depending on the function of the coordinate z (Figure 3). We accept the condition of incompressibility for the material of the sealing element, it will have the form:

$$\varepsilon_r + \varepsilon_j + \varepsilon_z = 0 \quad (4)$$

where: $\varepsilon_r, \varepsilon_j, \varepsilon_z$ – are respectively relative radial, tangential and axial deformation of any point of the sealing element.

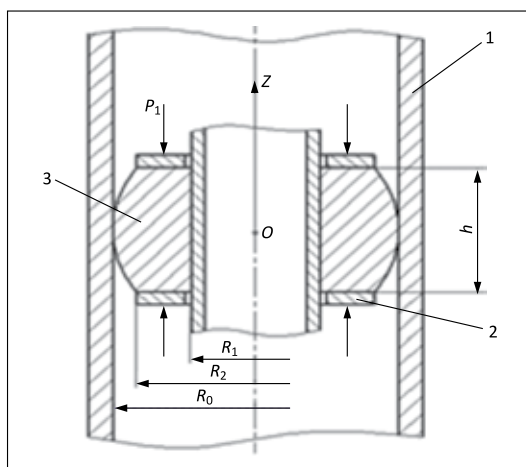


Figure 3. Scheme of deformation of the sealing element: 1 – support sealing, 2 – support washer, 3 – sealing for rubber

Rysunek 3. Schemat odkształcenia elementu uszczelniającego: 1 – uszczelka obudowy, 2 – podkładka obudowy, 3 – uszczelnienie gumowe

During operation, the sealant is loaded with external pressure (P) and internal pressure (q) arises in the seal body, obtained in a stressed equilibrium state (Guliyev and Sharifova, 2019). Let us determine the pressures P and q necessary to maintain the elastic element in an elastic state.

For this, we compose a differential equation of the equilibrium state, and, at the same time, we accept the case when ($\varepsilon_j = \text{const}$), and in this case the packer channel is pressed only by internal pressure (Mammadov et al., 2016):

$$\frac{d\sigma_r}{dr} + \frac{\sigma_r - \sigma_\theta}{r} = 0 \quad (5)$$

For such a flow condition, i.e., leakage, will:

$$\sigma_r - \sigma_\theta = 2K_3 \sigma_{seal}$$

where: $K = K_{h,f}$ – in this case, the filling factor, taking into account the thermal field, the exponential terms can be expanded into a series and the term linear in h can be saved, we get (Hasanov, 2016):

$$K_{h,f} = K_3 \exp[-\kappa T]; K_3 = V_p / V_\kappa \text{ at } T = T_0 \quad (6)$$

$$P = \frac{Q \cdot \Delta h}{2V_p} = \sigma_{el,d}; \quad q = \frac{M_Q S_a}{V_p} = \sigma_{el,d} \quad (7)$$

where:

P – axial force acting on the seal,

Δh – axial deformation of the elastic element,

V_p – compaction volume,

$\sigma_{el,d}^*$ – elastic deformation energy of the element, which is accumulated in the process of compaction,

M_Q – is the scale of the compression force,

κ – is the piezometric coefficient of volumetric expansion of the sealant at temperature T , according to the studies of many authors, $\kappa = 1$ is accepted,

S_a – the area of this curve and the abscissa axis are predetermined by the trapezoid formula or experimentally.

For the design of a new seal assembly in downhole equipment, in most cases, the internal diameter of the production string is set – D , T is the temperature of the medium, the pressure drop in the seal. Assuming the following initial data: $T = 373\text{--}393$ K; $D = 152$ mm – packer channel, the value of which is taken according to industry standards for downhole devices. Determine the fill factor:

$$K_{h,f} = K_3 \exp[\kappa T] = V_p / V_\kappa \exp[\kappa T] = 0.95$$

$\kappa = 3\alpha_{ex,c}$ – coefficient of volumetric expansion of rubber; for a rubber material is defined as follows:

$$\alpha_{ex,c} = 3/\kappa = 1.78 \cdot 10^{-1} 1/s;$$

$\frac{\sigma_{el,d}^*}{E_{comp}} = 0.172$; $E_{comp} = 3.863$ MPa (Dzhanakhmedov, 1998)

Considering the mechanical characteristics of the seal (E_{comp} – compression modulus of rubber), the last equation can be represented in a dimensionless form (Hasanov et al., 2020).

$$L_V = \frac{V_p}{V_k} \exp[\kappa T] \ln \frac{R_k^2}{R_{seal}^2} \cdot \frac{\sigma_{seal}}{E_{comp}} + \frac{M_Q S_n}{V_p E_{well}} \quad (8)$$

When $R_2 = R_k$ seals are in operation, where R_k is the radius of the inner wall of the column; radius of rubber (seal) is $R_{20} = R_p$ (Dzhanakhmedov, 1998):

$$R_1 = R_{10} = R_{el-d}$$

From here:

$$R_k = R_p; \quad V_p = V_k$$

$\sigma_{seal} = 0.666$ MPa – determined experimentally for a given compaction (Osipov et al., 2014):

$$\frac{M_Q S_n}{V_p E_{well}} = \frac{\sigma_{el-d}^*}{E_{comp}} = 0.172$$

Considering the above limit value L_V , the axial force on the seal will be:

$$L_V = 0.95 \frac{0.666}{3.863} \ln \frac{(7.6)^2}{(5.0)^2} + 0.172 = 0.309$$

Calculations show that the amount of leakage of the elastic elements in the sealing unit should not exceed:

$$L_V = \frac{Q \Delta h}{2 V_p E_{comp}} \leq 0.309$$

a compaction at the value of elastic energy deformation;

$$\frac{\sigma_{el-d}^*}{E_{comp}} = 0.172$$

provides self-compacting mode.

Thus, the equation of the equilibrium stress-strain state of the downhole packer sealing unit is determined, considering the volumetric characteristics and mechanical properties of the seal. An equilibrium state in the sealing unit, between the proposed force and the sealing pressure and the internal pressure, has been found to determine the conditions that ensure the protection of the elastic elements of the well sealant from leakage.

As is known, one of the factors that significantly affect the operation of pumps is fluid leakage in valve assemblies. To determine the fluid leakage in the valve units of a downhole rod pump, the following functional relationship is considered:

$$Q = f(\eta, h, \Delta p, D) \quad (9)$$

where:

Q – is the fluid flow through the gap between the seat and the ball,

η – liquid flow rate in case of leakage,

h – is the height of the late landing of the ball on the valve seat,

Δp – pressure drop across the valve,

D – diameter of the working chamfer of the seat.

To identify the effect of the above parameters on the tightness of the valve, based on a preliminary theoretical analysis, it was found that the fluid flow through the gap between the seat and the ball during the transition process can be represented as the following formula (Urbanovich, 2000):

$$Q = \frac{\pi}{2} \cdot \eta (D_0 + D_k) H \sqrt{\frac{2g\Delta p}{\gamma}} \quad (10)$$

Here: H – is the height of the maximum lift of the ball,

D_k and D_0 – are the diameters, respectively, of the circumference of the spherical segment enclosed between the perpendiculars, lowered from the center of the ball by the diameter of the working chamfer of the valve seat at the current and full rise to heights h and H , respectively.

The experiment was conducted on an oil product with dynamic viscosities from $\mu = 1.095$ to 5.73 Pa·s. It follows from this that the filling factor of the pump at high viscosities is greater than at low viscosities. Comparison of data during the study showed that the flow rate, when working with low viscosities, is greater than with high ones.

The experimental data were processed by the regression analysis method according to the following formulas (Mildin et al., 2011):

$$\eta = b_0 \left(\frac{h}{D} \right)^{b_1} \quad (11)$$

$$b_1 = \frac{\sum_{i=1}^N \ln \left(\frac{h}{D} \right)_i \sum_{i=1}^N \ln(\eta)_i - N \sum_{i=1}^N \ln \left(\frac{h}{D} \right)_i \ln \eta_i}{\sum_{i=1}^N \ln \left(\frac{h}{D} \right)_i^2 - N \sum_{i=1}^N \ln \left(\frac{h}{D} \right)_i} \quad (12)$$

$$b_0 = \exp \left[\frac{1}{N} \left(N \sum_{i=1}^N \ln \eta_i - b_1 N \sum_{i=1}^N \ln \left(\frac{h}{D} \right)_i \right) \right] \quad (13)$$

where:

N – is the number of observations,

η – is the consumption coefficient determined by observation.

After appropriate mathematical processing of the experimental data for the above pumps, it has been determined that the calculated coefficients of liquid flow rate in case of leakage can be expressed by the relation:

$$\eta_p = 0.2698 \left(\frac{h}{D} \right)^{-1.4286} \quad (14)$$

Table 3. The data obtained during the study and calculated by formulas (14)**Tabela 3.** Dane uzyskane w czasie badania oraz obliczone przy pomocy wzorów (14)

h/D	0.10	0.12	0.14	0.16	0.18	0.22	0.25	0.30	0.36	0.42
η	6.80	5.25	4.20	3.47	2.90	2.20	1.84	1.40	1.09	0.87
η_p	7.00	5.40	4.30	3.50	3.02	2.20	1.89	1.42	1.10	6.90

The data obtained during the study and calculated by formulas (14) are presented in Table 3.

Do and Dk are defined constructively. The height of the late landing of the ball on the seat was obtained experimentally. The pressure at the pump intake can be determined by the formula

$$P_i = \frac{(H_p - H_g)\gamma}{10} \quad (15)$$

where:

H_p – is the depth of the pump suspension,

H_g – is the dynamic level of the liquid.

$$H_g = L_{well} - \frac{10P_b}{g} \quad (16)$$

L_{well} – well depth, P_b – bottom hole pressure. Jointly solving equation (15) and (16) we obtain:

$$P_{trans} = P_b - \frac{L_{well}\gamma}{10} + \frac{H_{\Pi}\gamma}{10} \quad (17)$$

After a simple transformation of equation (10), taking into account (17), we have:

$$Q = \frac{k}{2}\eta(D_0 - D_k)h \cdot \left\{ \frac{2g[P_b + (L_{well} - 2H_p)\gamma]}{10\gamma} \right\}^{\frac{1}{2}} \quad (18)$$

With known parameters of the well, the pumped liquid and the valve, formula (18) makes it possible to determine the leakage with a delay in the landing of the ball on the valve seat.

Let us determine the amount of fluid leakage through between the working friction surfaces of the plunger and the cylinder. With laminar flow of fluid in the gap, the amount of leakage is calculated using the following empirical formula.

$$q = 0.016g \frac{D_H H \delta^2}{\nu l} \quad (19)$$

where:

q – is the daily fluid leakage through the plunger-cylinder gap [m^3/day],

g – is the free fall acceleration, 9.81 cm/s^2 ,

D_H – pump diameter [cm],

δ – is the gap between the plunger and the cylinder [cm],

H – is the head created by the pumped liquid column, the height from the reduced dynamic level in the well to the wellhead, plus the backpressure at the wellhead [m],

ν – is the kinematic viscosity of the pumped liquid [cm^2/s],

l – is the contact length of the working surfaces of the cylinder and plunger [m].

The formula is approximate since it does not consider the effect of the increase in fluid by the plunger as it moves up. From the formula, it follows that the leakage is directly proportional to the diameter of the pump and the height of the liquid. The smaller they are, the greater the viscosity of the pumped liquid and the length of the plunger. Currently, the pump I group is being produced with a gap of 0.01–0.0225 mm.

Let us calculate the leakage formula in a new 55 mm pump II group with a gap of 0.05 mm, i.e., 0.005 cm under average operating conditions: $H = 600 \text{ m}$, $\nu = 0.03 \text{ cm}^2/s$ and the standard contact length of the working surfaces of the pair $l = 1.2 \text{ m}$:

$$q = 0.016 \cdot 981 \frac{5.5 \cdot 600 \cdot 0.005^2}{0.03 \cdot 1.2} = 0.18 \text{ m}^3/\text{day}$$

The delivery of a new 55 mm pump averages approximately $35 \text{ m}^3/d$. This means that the leakage will be from the actual supply of the pump:

$$0.18/35 \approx 0.005 \text{ or } 0.5\%$$

Therefore, hydraulic gap sealing can be quite effective. Moreover, it should be considered that, for the normal operation of the pump, lubrication of the rubbing surfaces of the plunger and cylinder is necessary, and therefore small fluid leaks are inevitable (Figure 4).

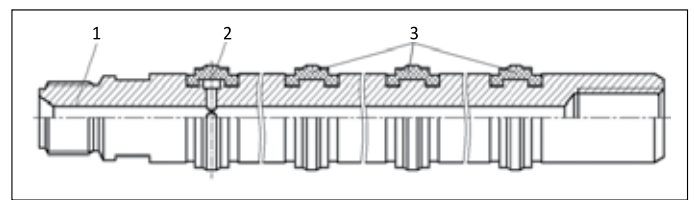


Figure 4. The design of the sleeve plungers of borehole pumps; 1 – plunger body; 2 – rubber ring, 3 – swelling rubber rings

Rysunek 4. Konstrukcja nurników tulejowych pomp głębinowych; 1 – korpus nurnika; 2 – pierścień gumowy, 3 – pęczniące pierścienie gumowe

The operating conditions of X-mas trees have their own specific features that differ from other machines and equipment (Figure 5):

The ovality of the outer and inner diameters was less than 0.3 mm. The deviation from the joined outer and inner diameters is characterised by the value Δ_a . (Figure 6.) The value Δ_a ranged from 0.05 to 0.9 mm. Ten springs had $\Delta_a > 0.4 \text{ mm}$,

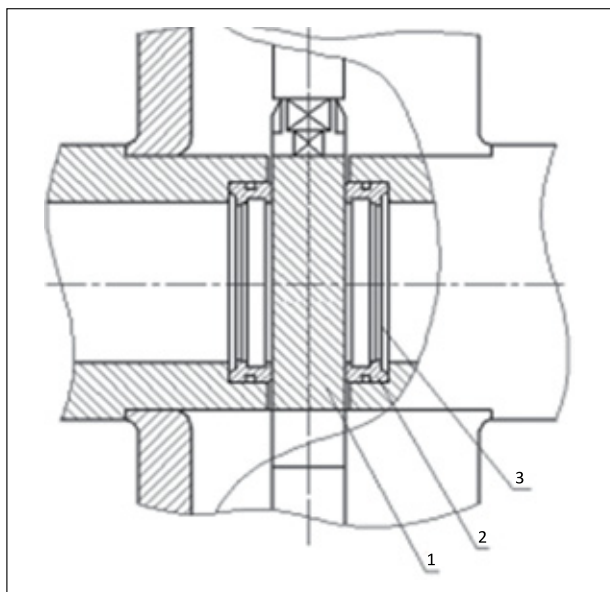


Figure 5. Valve operating unit; 1 – seat, 2 – gate, 3 – disk spring
Rysunek 5. Zespół roboczy zaworu; 1 – gniazdo, 2 – zasuwka, 3 – sprężyna talerzowa

DH and dH nominal outer and inner diameters of the spring. H and S are the nominal height and thickness of the spring, respectively (Androno et al., 2008; Zimmermann et al., 2015).

For the spring, according to the drawing: $DH = 83.5$ mm, $dH = 71$ mm, $H = 4.5$ mm, $S = 2$ mm and $\alpha = 26^\circ 30'$. From Figure 6 it follows that $\Delta H = \Delta_a \cdot \operatorname{tg}\alpha$; $H_{\max} - H_{\min} = 2\Delta_a \cdot \operatorname{tg}\alpha$, $\operatorname{tg}26^\circ 30' = 0.05$ and therefore for the considered spring $H_{\max} - H_{\min} = \Delta_a'$ i.e., the non-parallelism of the ends of the spring is numerically equal to the misalignment value Δ_a .

The value $H_{\max} - H_{\min} = \Delta_a$ determines the degree of uneven pressure of the seat against the gate. When the spring is deformed, an off-center elastic force of the spring occurs, which is determined by the value Δ_a . This force rotates the seat, increasing the probability of it jamming in the body and tearing off the seat surface on the gate, i.e., non-tolerance (Δ_a) worsens the sealing of the mating surfaces of the seat and gate. Thus, at $\Delta_a = 0.4$ mm, the non-central elastic force will be 320 kGf and the moment of this force is ≈ 10 kGf·m, i.e., very significant values (Goren et al., 2013; Nermoen et al., 2013).

It is considered that the value Δ_a should be less than 0.1 mm. To fulfill this condition, it is proposed to increase the accuracy of processing the outer diameter of 11 grades and reduce the runout of the mandrel for boring the inner diameter to 0.05 mm.

The non-flatness of the supporting end of the spring did not exceed 0.2 mm, and for forty springs it was less than 0.1 mm. The thickness of the spring material ranged from 2 ± 0.05 mm for 37 springs and $2_{-0.05}^{+0.2}$ at 13 springs.

Table 4 shows the calculation data for the operational values of spring compression for various material thicknesses. The thickness of the spring has a significant effect on the elastic

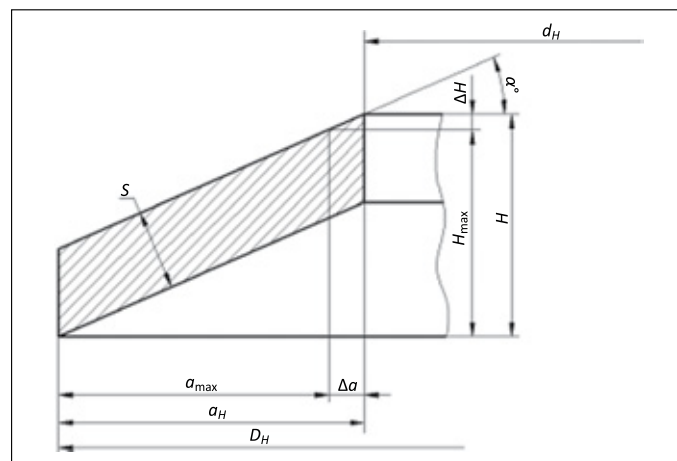


Figure 6. Scheme for calculating spring height deviations
Rysunek 6. Schemat obliczania odkształceń wysokości sprężyny

forces, however, at maximum values ($S = 2.2$ mm); this force is less than 10% of the force of pressing the seat to the slide valve caused by a hydrostatic pressure of 21 MPa (pressing force of more than 12 Tf). The height of the spring H depends on the tolerance field for the values DH , dH , S and α (Figure 6).

$$H = \frac{D-d}{2} \cdot \operatorname{tg}\alpha + \frac{S}{\cos\alpha} \quad (20)$$

For the springs under consideration, the calculated height of the springs can vary from 4.5 to 5.5 mm. The ends of the springs are not processed at the factory and the reference planes are sharp edges; the height of the springs ranged from 4.8 to 5.5 mm. Sharp edges violate the normal elastic deformation of the spring, cutting into the bearing surface of the nozzle (Megawati et al., 2012).

Table 4. Calculation data for operating values of spring compression for various material thicknesses

Tabela 4. Dane obliczeniowe dla wartości roboczych ścisnięcia sprężyny dla różnych grubości materiału

Spring material thickness, S [mm]	Compression force kGf at 1.3 mm spring deformation	Compression force kGf at 1.8 mm spring deformation
1,95	693	792
2,00	736	848
2,05	782	907
2,10	829	968
2,15	879	1032
2,20	930	1100

The springs are quenched in a flame gas furnace, followed by tempering in an electric furnace. Ovality, due to warping of the springs, increased in ten springs to 0.5 mm or more. Experiments have shown that the use of the simplest equip-

ment for assembling springs in stacks for heating for hardening practically eliminates their warpage.

The hardness of the springs after heat treatment was 42–49 HRC.

Consideration of the data on the properties of reinforcing layers given in the literature sources allows us to choose, as the main ones for further research on the hardening of parts from grades 40, 40X and 38X2MA1A of the locking unit of direct-flow valves, the following technological processes of chemical-thermal treatment: nitro carburizing in a triethanolamine medium during induction heating with high frequencies, single-phase boriding, two-phase boriding, boriding + chromium plating (borochrome plating). The selected hardening methods are relatively simple and accessible and have good wear resistance under extreme operating conditions.

Thus, with a high appearance, the influence of the height of the spring on its elastic properties was established; the residual deformation after filling reduced the height of the spring mainly to 3.7... 4.2 mm and, as a result, elastic deformation of the spring reduces to 0.8... 0.3 mm resources corresponding to the pressing force of the seat against the slide valve. It was determined that only springs with a height of 4.3 mm in their parameters approach those calculated according to GOST and can sufficiently ensure the sealing of the shut-off valve assembly at low pressures of 3... 5 MPa. It should also be noted that the nature of the change in the dependence “force-deformation” and with various deformations correspond to changes in the calculated characteristics.

Conclusions

1. The exploitation of the work of the elastic elements of the packer was conducted mainly constructively, and the optimal parameters for the development of the elastic element of the packer have been determined. The study of the stress-strain state of the sealing element of packers during setting and improving its performance is of both practical and scientific interest.
2. Calculations (9) show that the amount of leakage of the elastic elements in the sealing assembly should not exceed $P_z \leq 0.309$, since the seal at the value of elastic $\sigma_{el.d}^*/E_{comp} = 0.172 = 0.72$ provides self-compacting mode.
3. One of the factors that significantly affects the operation of the pumps is the leakage of liquid in valve assemblies to identify the effect of the above parameters on tightness based on a preliminary theoretical analysis. Comparison of data during the study showed that the flow rate with low viscosities is greater than with high viscosities.

4. Technological processes of hardening the parts of the shut-off assembly of X-mas tree valves, in order to increase their reliability, are considered. The dependence of the compression force of the spring and its deformation on the geometric parameters of the disk springs has been found; it has been determined that the residual deformation of the disk spring after collapse has a negative effect on tightness.

References

- Androno I.N., Kuzbogev A.S., Aginey R.V., 2008. Resource of ground pipelines – I: Factors that constraining resource. *Standard Test Methods, Ukhta*, 75–96.
- Babanli M., 2016. Impact of thermoplastic deformation on work of rotating preventers sealing and others. *Science and Education: Materials of the XII International Research and Practice Conference, Germany*, 42–54.
- Disk springs, 2003. General specifications: GOST 3057-90. *IPK Publishing House of Standards*, 37.
- Dzhanakhmedov A.Kh., 1998. Tribological problems in oil and gas equipment. *ELM, Baku*, 216.
- Goren L., Toussaint R., Aharonov E., Sparks D.W., Flekkøy E., 2013. A General criterion for liquefaction in granular layers with heterogeneous pore pressure. *Poromechanics V: Proceedings of the Fifth Biot Conference on Poromechanics*. DOI: 10.1061/9780784412992.049.
- Guliyev A.A., Sharifova A.V., 2019. Study of the influence of geometric parameters and thermal technology on the residual deformation and elastic properties of disk springs. *Oil and Gas Technologies and Analytics, Moscow*, 58–62.
- Hasanov I.I., 2016. Assessment of vibration influence on packing system of Christmas tree. *Journal of Modern Science*, 7: 18–22.
- Hasanov I.I., Abbasov I.I., Gurbanov N.A., 2020. Stress-Deformed State of a Packing Ring with Eccentric Holes. *Proceedings of the Latvian Academy of Sciences. Section B. natural, Exact, and Applied Sciences*, 74(4): 287–292. DOI: 10.2478/prolas-2020-0044.
- Mammadov V.T., Akhmedov A.S., Aslanov J.N., 2016. Investigation of stress-deformed state of coated hydrocylinders, exposed to pressure and temperature changes. *International Journal of Current Research*, 08(12): 44212–44216.
- Megawati M., Hiorth A., Madland M.V., 2012. The impact of surface charge on the mechanical behaviour of high-porosity chalk. *Rock Mechanics and Rock Engineering*, 46: 1073–1090. DOI: 10.1007/s00603-012-0317-z.
- Mildin A.M., Zelentsov D.G., Olevskiy V.I., Pletin V.V., 2011. Developing the concept of prediction the mechanical properties of thin-walled shells. *Eastern-European Journal of Enterprise Technologies*, 1(3): 57–61. DOI: 10.15587/1729-4061.2011.1902.
- Nermoen A., Korsnes R.I., Christensen H.F., Trads N., Hiorth A., Madland M.V., 2013. Measuring the Biot Stress Coefficient and Its Implications on the Effective Stress Estimate. *47th US Rock Mechanics, Geomechanics Symposium*, 1.
- Osipov T.N., Nesterov A.P., Rodinov L.A., 2014. Dissipation coefficient of a rubber-metal damping device in hoist ropes. *Machine Building*, 14: 24–29.
- Urbanovich V.S., 2000. Functional Gradient Materials and Surface Layers Prepared by Fine particles Technology. *ISM NASU, Kiev, Ukraine*, 169.

Zimmermann U., Madland M.V., Nermoen A., Hildebrand-Habel T., Bertolino S.A.R., Hiorth A., Korsnes R.I., Audinot J-N. Gysan P., 2015. Evaluation of the compositional changes during flooding of reactive fluids using scanning electron microscopy,

nano-secondary ion mass spectrometry, x-ray diffraction, and whole rock geochemistry. *AAPG Bulletin*, 99(5): 791–805. DOI: 10.1306/12221412196.



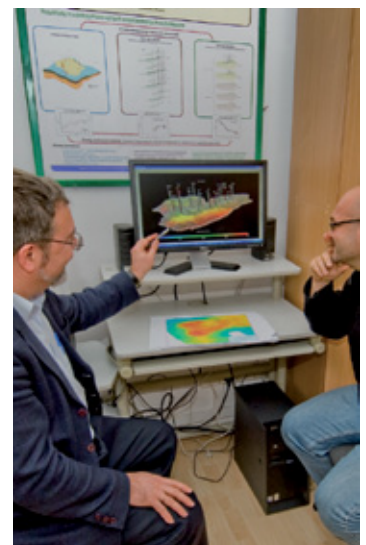
Ilman Iman HASANOV, Ph.D.
Assistant professor at the Department of Material Science and Processing Technologies
Azerbaijan State Oil and Industry University
16/21 Azadliq Ave, Baku, Azerbaijan
E-mail: hesenov.74@inbox.ru



Agali Ahmed GULIYEV, Ph.D.
Assistant professor at the Department of Material Science and Processing Technologies
Azerbaijan State Oil and Industry University
16/21 Azadliq Ave, Baku, Azerbaijan
E-mail: aaquliyev@mail.ru

OFERTA BADAWCZA ZAKŁADU SYMULACJI ZŁÓŻ WĘGLOWODORÓW I PMG

- sporządzanie ilościowych charakterystyk złóż naftowych (konstruowanie statycznych modeli złożowych);
- analizy geostatystyczne dla potrzeb projektowania modeli złóż naftowych, w tym PMG i wielofazowych obliczeń wolumetrycznych;
- konstruowanie dynamicznych symulacyjnych modeli złóż i ich kalibracja;
- wszechstronne badania symulacyjne dla potrzeb:
 - ✦ weryfikacji zasobów płynów złożowych,
 - ✦ wtórnych metod zwiększania wydobywania (zatlaczanie gazu lub wody, procesy WAG, procesy wypierania mieszającego, oddziaływanie chemiczne),
 - ✦ optymalizacji rozwiercania i udostępniania złóż,
 - ✦ prognozowania złożowych i hydraulicznych (w tym termalnych) charakterystyk odwiertów (w szczególności poziomych) dla celów optymalnego ich projektowania,
 - ✦ sekwestracji CO₂;
- projektowanie, realizacja i wdrażanie systemów baz danych dla potrzeb górnictwa naftowego.



Kierownik: dr inż. Piotr Łętkowski
Telefon: 13 434 96 29

Adres: ul. Armii Krajowej 3, 38-400 Krosno
Faks: 13 436 79 71 E-mail: letkowski@inig.pl



INSTYTUT NAFTY I GAZU
– Państwowy Instytut Badawczy